

INFLUENCE OF DISLOCATION STRUCTURE ON DEFORMATION PROCESSES IN AlGaN/GaN/(0001)Al₂O₃ HETEROSTRUCTURES

V.P. KLADKO, A.V. KUCHUK, N.V. SAFRYUK, A.E. BELYAEV,
V.F. MACHULIN

PACS 61.05.C, 61.46.-w, 61.72.Dd, 61.72.Ff, 62.20.F, 65.80.+n
©2009

V.E. Lashkarev Institute of Semiconductor Physics, Nat. Acad. of Sci. of Ukraine
(45, Nauky Ave., Kyiv 03028, Ukraine)

The results of high resolution X-ray diffractometry (HRXD) studies of the structural properties of AlGaN/GaN/(0001)Al₂O₃ heterosystems are reported. The microscopic nature of spatial heterogeneities (microdeformations and the dislocation density) in those structures is discussed on the basis of the results obtained. The gradient distribution of dislocations and deformations over the structure depth both in the mosaic (block) structure of nitride layers and across the interface with the sapphire substrate has been confirmed by numerical simulation. The correlation between the deformation and the dislocation density in both the layers and the substrate with the variation of the substrate thickness has been established. In particular, the growth of sapphire substrate thickness has been demonstrated to result in an increase of dislocation density and a decrease of elastic deformations in the layers. The scenario of a connection between elementary cells of the layer and the substrate at the interface, which minimizes the lattice misfit, has been confirmed experimentally.

1. Introduction

III-nitrides should play an important role in the semiconductor industry for the creation of reliable light-emitting and laser diodes, as well as high-temperature and high-current electronic devices [1]. In spite of the rapid progress attained within last years in the technology of such devices, the growing of GaN still remains a problematic task. A large mismatch between the lattice constants and the coefficients of thermal expansion of III-nitrides and substrates, which are used for their growth (sapphire), provokes the growth of structurally imperfect epitaxial layers with a high concentration of structural defects (the dislocation density can achieve $10^8 - 10^{10} \text{ cm}^{-2}$) and considerable residual deformations [2–4]. The layers of III-nitrides grown on Al₂O₃ (0001) substrates have, as a rule, a mosaic structure consisting of nanocolumns (blocks) oriented along the *c*-axis [5, 6]. The absence of definitely established physical mechanisms, which would be responsible for the dependence of III-nitride properties on the mosaic (block) structure features, evidently constrains progress

in the technology aimed at the growing of such structures. The solution of a challenging problem dealing with the controlled improvement of the parameters of III-nitride-based heterostructures that are used in devices demands that the influence of a deformation state of nitride layers, the mosaic structure, and defects that are formed at the relaxation of elastic deformations on optical and electric properties should be studied in detail.

It is known [7–9] that X-ray diffractometry is an effective method for the determination of structural parameters averaged over the volume, elastic deformations, and the component composition of nitride structures. In addition, the analysis of X-ray rocking curves in various diffraction geometries and two-dimensional maps of the intensity distribution around reciprocal lattice sites allows one to characterize the orientational distribution of structural defects [10–14]. Therefore, the purpose of this work was to use X-ray diffractometry to study the influence of the dislocation density, type, and distribution on the deformation state and the relaxation mechanism in AlGaN/GaN/Al₂O₃ heterostructures and the dependences of those quantities on the sapphire substrate thickness.

2. Experimental Technique

We studied epitaxial AlGaN/GaN heterostructures grown by the method of metallo-organic chemical vapor deposition (MOCVD) onto substrates made of sapphire Al₂O₃ with orientation (0001) and 450 and 3000 μm in thickness (hereafter, thin and thick substrates, respectively). First, a 3- μm buffer layer of GaN was grown on a sapphire substrate, then, a layer of Al_{0.30}Ga_{0.70}N about 30 nm in thickness, which was then covered with a GaN layer about 4 nm in thickness. The angular misorientation of substrate surfaces did not exceed 30'.

The X-ray diffraction studies of specimens were carried out on a “PANalytical X’Pert PRO MRD” diffractometer. The symmetric (0001) and asymmetric (10-12) and (-1-124) reflections were analyzed. The experimental schemes allowed two cross-sections of reciprocal lattice sites to be obtained: normally (ω -scanning) and in parallel ($\omega/2\theta$ -scanning) to the diffraction vector. The application of the asymmetric Bragg geometry allowed the properties of symmetric Bragg and Laue diffractions to be combined. Since triaxial diffractometry is capable of distinguishing between the effects associated with a variation of the interplane distance and a rotation of atomic planes, the analysis of the intensity distribution in a coordinate system (q_z, q_x) with the axes oriented along and normally to the diffraction vector \mathbf{Q} makes it possible to determine each of those contributions separately [15]. The azimuthal Φ -scanning at asymmetric (11-2 l) reflections was used to determine a misorientation between GaN blocks in the growth plane and the substrate. Macroscopic deformations that were responsible for the specimen bending were estimated from the curvature radius of the system, which was determined by analyzing a variation of reflection angles from sapphire at the linear scanning of a specimen along the X-ray beam [16]. Since the layers were much thinner than the substrate, the curvature radii of the layer and the substrate were considered to be identical.

3. Experimental Results

In Fig. 1, the two-dimensional reciprocal space maps (RSMs) of the intensity distribution around (0002) and (-1-124) sites for the heterostructures under investigation are depicted. The RSMs demonstrate two reflection centers: from GaN and AlGaN films. The reflection maxima from the sapphire substrate are not shown, because they are located far, by the angular position, from the films. From Fig. 1, it is evident that the layers are strained, because the interference pattern of intensity distribution along a normal to the surface is observed for both symmetric (Figs. 1,*a* and *c*) and asymmetric (Figs. 1,*b* and *d*) reflections. In both cases, the contours of intensity distribution are elongated normally to the vector \mathbf{Q} . Since the influence of dislocation networks on Bragg diffraction is reduced to a broadening of the diffraction pattern in the direction normal to the diffraction vector \mathbf{Q} and practically does not affect the intensity distribution along the diffraction vector, such an intensity distribution observed on RSMs is characteristic of structures with non-relaxed elastic deformations and misfit dislocations [17].

In order to determine microdeformations in the blocks of mosaic structure – the coherent scattering regions (CSRs) – and their dimensions, the Williamson–Hall method [18, 19] was used. The broadening of ω -scans (they are characterized by the halfwidth β_Ω) of symmetric reflections is affected by the block slopes α_Ω and the lateral correlation length L_\parallel :

$$\beta_\Omega = 0.9 / (2 L_\parallel) + \alpha_\Omega, \quad (1)$$

On the other hand, the broadening of $\omega - 2\theta$ -scans (the halfwidth is β) corresponding to symmetric reflections is connected with the vertical correlation length L_\perp and the magnitude of inhomogeneous microdeformations along the growth direction, ε_\perp , being determined by the formula

$$\beta = 1 / (L_\perp) + 2 \varepsilon_\perp Q. \quad (2)$$

On the basis of Eqs. (1) and (2), one can see that the dependences of the reflection curve halfwidths on the diffraction vector are linear. The slopes of the corresponding straight-line plots are associated with the contribution made by microscopic misorientations and microdeformations, whereas their intersections with the ordinate axis correspond to the CSR dimensions in two mutually orthogonal directions.

The slopes of dependences (1) describe the distribution of block misorientations with respect to the surface normal which originate from the presence of screw dislocations with the Burgers vector $b_s = [0001]$ (in our case, $|b_s| = 0.5185$ nm). Their density can be estimated from the relation [18]

$$N_S = \frac{\alpha_\Omega^2}{4.35 b_S^2}. \quad (3)$$

The density of edge dislocations with the Burgers vector $b_E = 1/3\langle 1120 \rangle$ ($|b_E| = 0.3189$ nm) in the slip planes $\{1-100\}$, which makes the blocks to rotate, was determined on the basis of the asymmetric scan broadening α_Φ using the formula

$$N_E = \frac{\alpha_\Phi^2}{4.35 b_E^2}. \quad (4)$$

The values of the parameters for AlGaN/GaN structures grown up on thin and thick sapphire substrates, which were determined making use of formulas (1)–(4), are listed in Table 1. In the case of GaN layers grown up on a thick substrate, the CSR dimensions along the structure growth direction (the block heights) are twice as large as those for the layers on a thin substrate. At

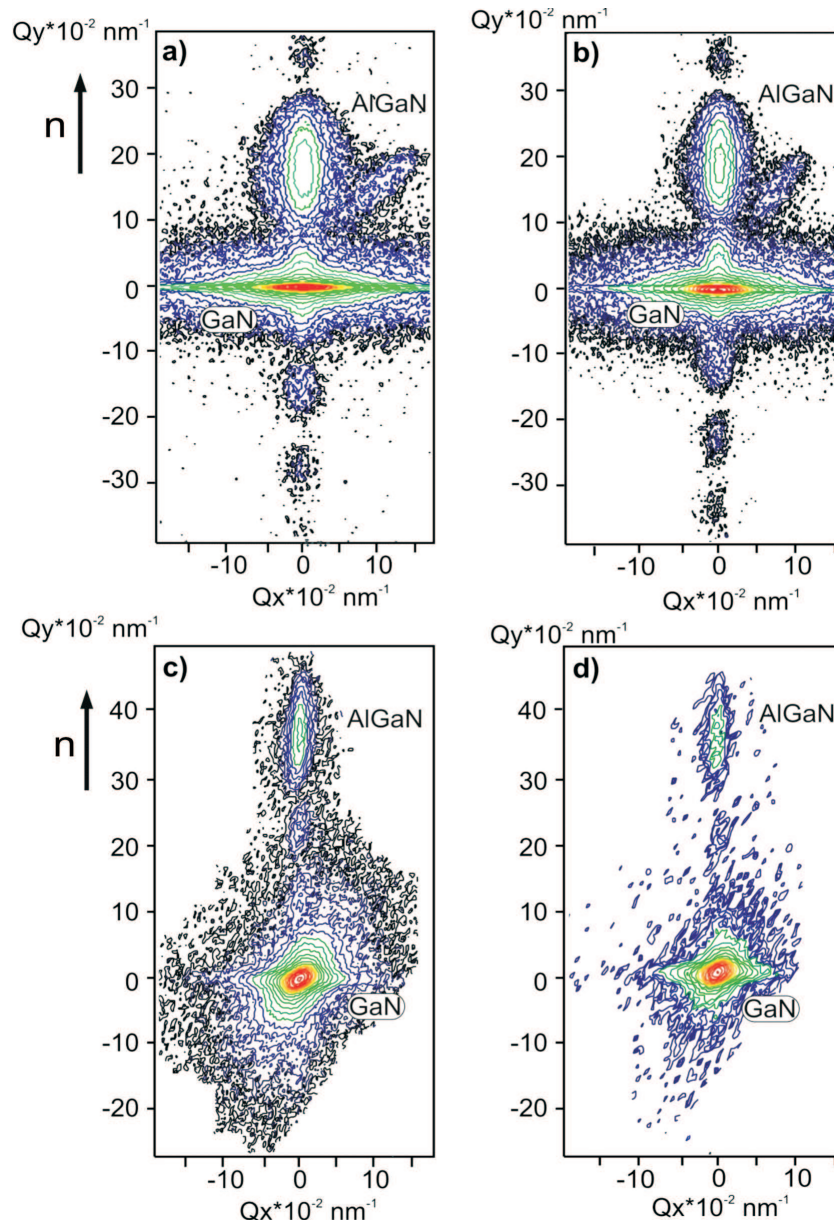


Fig. 1. Two-dimensional maps of the intensity distribution around of nodes (0002) (panels *a* and *c*) and (-1-124) (panels *b* and *d*) for heterostructures grown up on thin (*a* and *b*) and thick (*c* and *d*) substrates; *n* is the surface normal

T a b l e 1. X-ray experimental structural parameters for AlGaIn/GaN structures grown up on thin and thick sapphire substrates

Substrate thickness (μm)	Layers	ε_{\perp}	CSR dimensions (nm) L_{\parallel}/L_{\perp}	Dislocation density ($\times 10^8 \text{ cm}^{-2}$) N_E/N_S	Curvature radius R (m) exp./calc.
450	GaN	9.04×10^{-4}	31.7/58.8	13.8/0.98	9.91/0.08
	AlGaIn	6.9×10^{-4}	21.7/29.9	2.54/2.9	
3000	GaN	3.04×10^{-4}	64.5/50.0	6.2/1.09	69.3/3.50
	AlGaIn	3.79×10^{-4}	20/38.3	2.8/1.74	

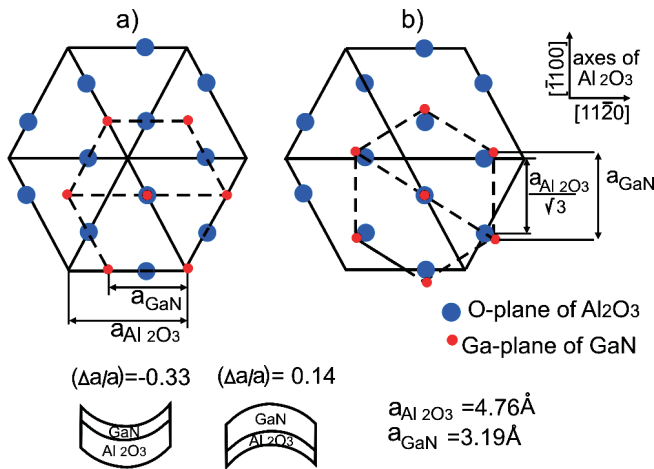


Fig. 2. Schematic diagram of the atomic arrangement in the growth plane and the bend of GaN/(0001)Al₂O₃ system at lattice parameter mismatches of -0.33 (a) and 0.14 (b)

the same time, in the case of AlGaN layers, the vertical dimensions of CSRs are practically identical in both structures, being equal to the geometric thickness of the layer. For GaN layers, the magnitudes of deformation parameters and the CSR dimensions correlate with the density of edge dislocations. The densities of screw or edge dislocations with the Burgers vector close to the growth-surface normal are practically the same for those two structures in the case of GaN layers. However, the component of the strain tensor ε_{\perp} for a GaN layer on a thin substrate is three times as large as that in the thick-substrate case. A similar relationship takes also place for AlGaN layers.

It is important to emphasize that the character of elastic deformation variations over the depth at the interface between the epitaxial layer and the sapphire substrate does not depend on the thickness of the latter, although elastic deformations are larger in nitride layers on a thick substrate. The measured curvature radii of both structures differ strongly from the corresponding calculated values (Table 1). This circumstance stimulated the study of the origins of this effect, because the relaxation of elastic deformations associated with the dislocation density cannot explain it alone.

4. Discussion of Results

The emergence of plane misorientations in the heterostructure is caused by the rotation of corresponding layers with respect to either a substrate or one another. The rotation of planes is caused by screw components of dislocations with the Burgers vector parallel to the

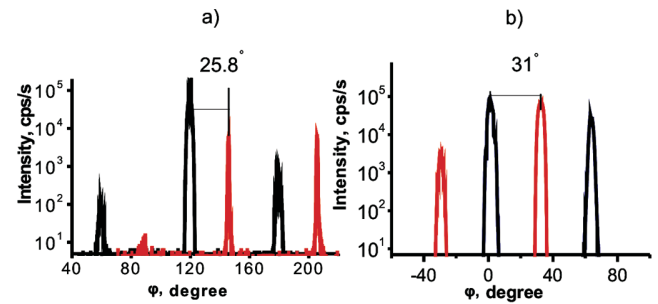


Fig. 3. Φ -scans around the surface normal for diffraction planes (11-24) of GaN films and (11-29) of sapphire substrates 450 (a) and 3000 μm (b) in thickness

heterointerface or by edge dislocations with the Burgers vector $b_E = 1/3\langle 1120 \rangle$. This is a direct confirmation of the theoretical concept that the macroscopic disorientation of layers with respect to the substrate originates from both the presence of a dislocation network and a deviation of the crystal surface from a regular crystallographic orientation [16].

Figure 2,a demonstrates that the mismatch between lattice parameters at the GaN/Al₂O₃ interface is $(\Delta a/a) = (a_{\text{GaN}} - a_{\text{Al}_2\text{O}_3})/a_{\text{Al}_2\text{O}_3} = -0.33$, where $a_{\text{GaN}} = 0.31876 \text{ nm}$ and $a_{\text{Al}_2\text{O}_3} = 0.4758 \text{ nm}$ [20]. In the course of coherent growth, such a discrepancy between the lattice constants has to induce a macroscopic bend of the substrate–epitaxial layer system, with the film side being concave. However, in our experiments, the system got bent in such a manner that the film surface turned out convex. This fact demands the explanation and confirmation.

Therefore, since the film has a column-like structure, we suppose that the effect described above may result from the fact that GaN blocks are arranged in the growth plane with a different (with the opposite sign) lateral mismatch (Fig. 2,b). The corresponding mismatch value $(\Delta a/a)_l = (a_{\text{GaN}} - a_{\text{Al}_2\text{O}_3})/a_{\text{Al}_2\text{O}_3} = 0.14$ ($a_{\text{GaN}} = 0.31876 \text{ nm}$ and $a_{\text{Al}_2\text{O}_3} = 0.2749 \text{ nm}$) can be obtained by rotating a GaN cell with respect to the sapphire one by an angle of 30° around the [0001] axis [21]. Experimentally, it manifests itself in that asymmetric reflections of type 11-2*l* are fixed for the layer and the substrate at different azimuthal orientations of the specimen (Fig. 3). We found that the lateral misorientation between GaN and sapphire cells amounts to about 25.8° and 31° for structures on thin and thick substrates, respectively. Such rotations may result from a higher density of dislocations with screw segments (the Burgers vector is parallel to the interface plane).

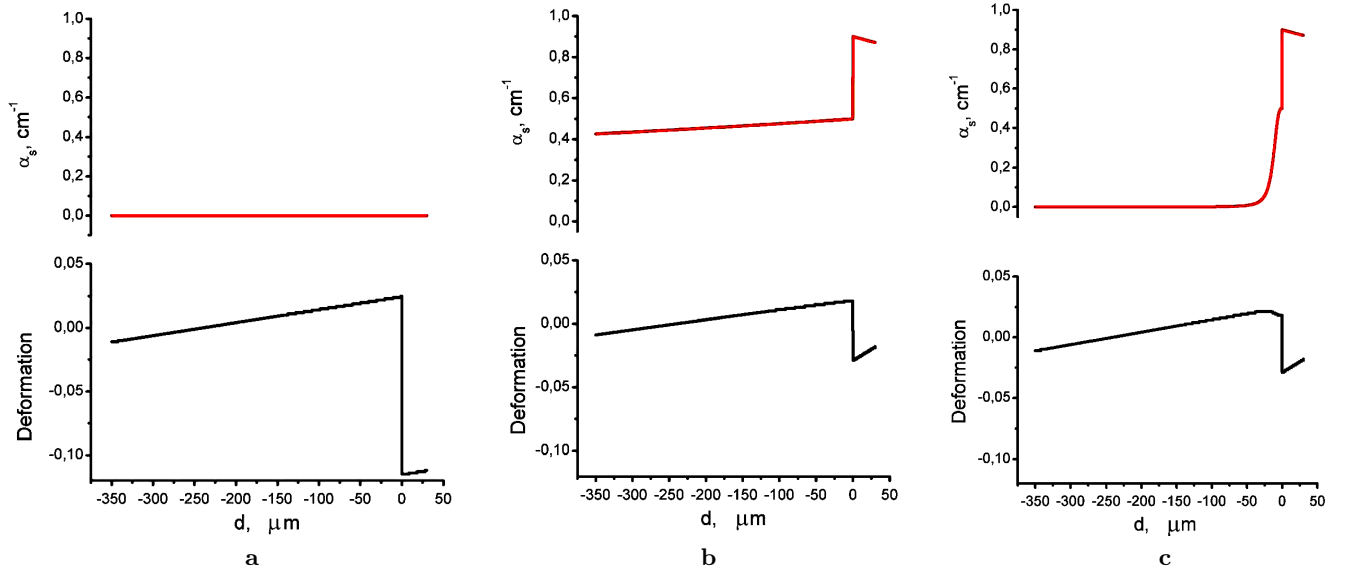


Fig. 4. Dependences of the deformation distribution on the density and the distribution law of dislocations in the structures: (a) without dislocations, (b) linear distribution, and (c) quadratic distribution

A mismatch of 0.14 between the lattices constants gives rise to a corresponding sign of the system bend that is observed in experiment. However, the experimentally measured curvature radii are strongly different from the calculated ones, even if we take this mismatch into consideration (Table 1). To elucidate the main reasons of such discrepancies, let us calculate the dependence of the elastic deformation distribution in the system over its thickness on various parameters. The distribution is determined by the formula [22]

$$\varepsilon(z) = -\varepsilon^0(z) + \int_0^d \varepsilon^0(z) dz + R^{-1} \left(z - \frac{d}{2} \right), \quad (5)$$

where the function $\varepsilon^0(z) = \sum_{i=1}^{n-1} f^{(i)} \vartheta(z - z_i)$ for internal deformations in the structure.

The deformation distributions for various dislocation densities and distribution laws in the structures are given in Fig. 4. According to the presented data, the deformation jump at the interface is an order of magnitude smaller for structures with dislocations in comparison with the case of dislocation-free ones. However, the structure curvature radius does not correlate with the dislocation density (Table 1).

In Fig. 5, the theoretical and experimental dependences of the system curvature radius on the substrate thickness for various distributions of dislocations in the layers are exhibited. The calculation of the structure

curvature was carried out using the formula

$$R^{-1} = \frac{12}{d^3} \int_0^d \varepsilon^0(z) \left(z - \frac{d}{2} \right) dz, \quad (6)$$

where $\varepsilon^0(z)$ is the internal structure deformation, d is the structure thickness, and R is the curvature radius of the system.

By connecting the dislocation density with the corresponding deformation $\varepsilon^0(z)$, it is possible to calculate the dislocation contribution to the extra bend. According to the results of work [23], this relation can be presented in the form

$$\alpha = \frac{R(d) - R_m}{R(d)R_m} \frac{d_1^3}{(3d_1 - 2d_2)d_2^2}. \quad (7)$$

The dislocation density N_D , necessary for the compensation of stresses that are responsible for the discrepancy in the structure curvature values, amounts to $3.76 \times 10^{12} \text{ cm}^{-2}$ for a thin substrate and $3.53 \times 10^{10} \text{ cm}^{-2}$ for a thick one, which is considerably larger than the experimental data obtained from the analysis of a rocking curve. As the data of other authors [22] testify, the amplitude of a deformation jump (the curvature radius) depends on the law of a dislocation distribution in the layers. Our calculations showed that taking this factor into account does not change the radius of a system bend essentially. The dependences of the system curvature radius on the dislocation density in the layers are given in

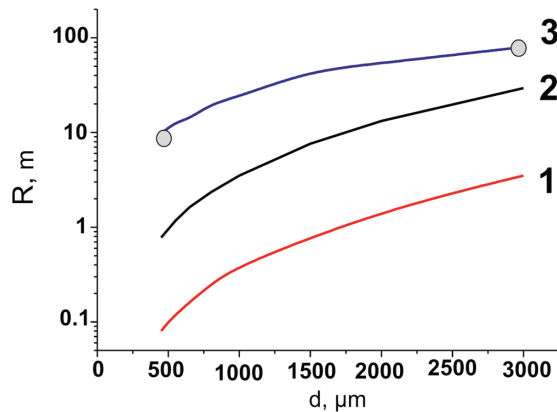


Fig. 5. Dependences of the structure curvature radius on the substrate thickness: perfect structure (1), with a uniform distribution of dislocations over the layer thickness (2), and taking into account the rotation of GaN cells with respect to sapphire. Points correspond to experimental data

Fig. 6. Hence, we see that the dislocation influence alone cannot explain the large discrepancy in the system bend.

In this connection, we also calculated the contribution of the volume fraction for each of cell orientations in order to elucidate whether a structure with a changed curvature can be obtained (the planar structure with zero curvature is obtained, provided that 30% of the volume is characterized by a mismatch of 0.14 and 70% by a mismatch of -0.33). It turned out that the cell rotation by 25° can really result in a reduction of the deformation jump at the system interface by a value of about 0.06 [24].

Thus, the difference between the values of deformation parameters for the layers in heterostructures grown up on “thin” or “thick” substrates mainly originates from different rotations of hexagonal cells, whereas the influences of the dislocation structures are equal. Such rotations are one of the mechanisms of elastic stress relaxation in the system, because they result in a reduction of the system curvature and, accordingly, macroscopic deformations. The role of thermal gradients is qualitatively similar to that of stresses associated with a lattice mismatch. However, the corresponding magnitudes are several orders smaller.

5. Conclusions

Structural researches of the $\text{Al}_{0.30}\text{Ga}_{0.70}\text{N}/\text{GaN}$ heterosystem showed that the main reasons for the broadening of X-ray reflections from these systems are disorientations – the so-called tilts and twists – and small

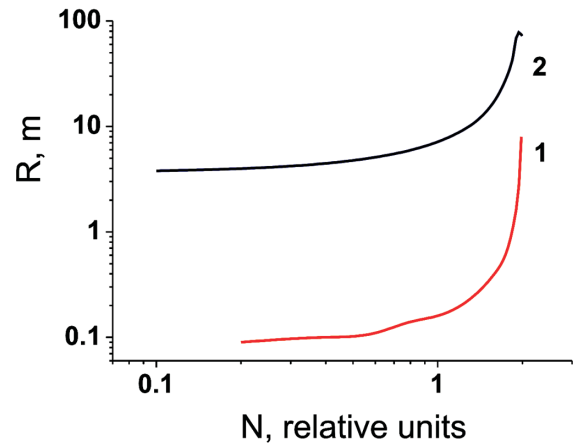


Fig. 6. Dependences of the structure curvature radius on the dislocation density at their uniform distribution over the layer depth for thin (1) and thick (2) substrates

dimensions of coherent regions. The observed broadening of the intensity distribution in parallel to the surface (perpendicularly to the diffraction vector) testifies that the dislocation ensemble consists of both the edge and screw components of dislocations with the Burgers vectors directed perpendicularly and in parallel to the heterointerface, respectively.

The presence of dislocations in A^3N heterostructures gives rise to a substantial redistribution of deformation fields in the blocks and macrodeformations (the macroscopic bend) with the variation of the sapphire substrate thickness. However, the complete agreement between the experimental and theoretical values for the system curvature can be achieved only provided that the rotations of blocks that compose the layer structures with respect to the substrate are taken into consideration.

The authors express their gratitude for given specimens and the fruitful scientific discussion to H. Hardt-degen and S.A. Vitusevich from the Institut für Bio- und Nanosysteme and the CNI-Center of Nanoelectronic Systems for Information Technology (Jülich, Germany).

1. T. Wang, J. Bai, S. Sakai, and J.K. Ho, *Appl. Phys. Lett.* **78**, 2617 (2001).
2. C. Kisielowski, J. Krüger, S. Ruvimov, and T. Suski, *Phys. Rev. B* **54**, 17745 (1996).
3. S.I. Cho, K. Chang, and M.S. Kwon, *J. Mater. Sci.* **42**, 3569 (2007).
4. S.D. Lester, F.A. Ponce, M.G. Craford, and D.A. Steigerwald, *Appl. Phys. Lett.* **42**, 3569 (2007).

5. Zh. Zhong, O. Ambacher, A. Link, V. Holy *et al.*, *Appl. Phys. Lett.* **80**, 3521 (2002).
6. L. Kirste, K.M. Pavlov, S.T. Mudie, V.I. Punegov, and N. Herres, *J. Appl. Crystallogr.* **38**, 183 (2005).
7. N. Herres, L. Kirste, H. Obloh, K. Köhler *et al.*, *Mater. Sci. Eng. B* **91–92**, 425 (2002).
8. M.A. Tagliente, L. Tapfer, P. Waltereit, O. Brandt, and K.-H. Ploog, *J. Phys. D* **36**, A192 (2003).
9. O. Brandt, P. Waltereit, and K.H. Ploog, *J. Phys. D* **35**, 577 (2002).
10. N. Herres, F. Fuchs, J. Schmitz, K.M. Pavlov *et al.*, *Phys. Rev. B* **53**, 15688 (1996).
11. V.V. Ratnikov, R.N. Kyutt, T.V. Shubina, T. Paskova, and B. Monemar, *J. Phys. D* **10**, A30 (2001).
12. V.P. Klad'ko, S.V. Chornen'kii, A.V. Naumov, A.V. Komarov, M. Tacano, Yu.N. Sveshnikov, S.A. Vitusevich, and A.E. Belyaev, *Semiconductors* **40**, 1060 (2006).
13. I. Kegel, T.H. Metzger, A. Lorke, J. Paisl *et al.*, *Phys. Rev. Lett.* **85**, 1694 (2000).
14. A. Krost, J. Blasing, F. Heinrichsdorf, and D. Bimberg, *Appl. Phys. Lett.* **75**, 2957 (1999).
15. P. Fewster, *X-Ray Scattering from Semiconductors* (Imperial College Press, London, 2000).
16. V.P. Kladko, A.F. Kolomys, M.V. Slobodian, V.V. Strelchuk, V.G. Raycheva, A.E. Belyaev, S.S. Bukalov, H. Hardtdegen, V.A. Sydoruk, N. Klein, and S.A. Vitusevich, *J. Appl. Phys.* **105**, 06351544 (2009).
17. B. Liu, R. Zhang, Z.L. Xie, H. Lu *et al.*, *J. Appl. Phys.* **103**, 023504 (2008).
18. R. Chierchia, T. Böttcher, H. Heinke, S. Einfeldt *et al.*, *J. Appl. Phys.* **93**, 8918 (2003).
19. T. Metzger, R. Hopler, E. Born, O. Ambacher *et al.*, *Philos. Mag. A* **77**, 1013 (1998).
20. V. Cimalla, J. Pezoldt, and O. Ambacher, *J. Phys. D* **40**, 6386 (2007).
21. S.C. Jain, M. Willander, J. Narayan, and R.V. Overstraeten, *J. Appl. Phys.* **87**, 965 (2000).
22. Yu.A. Tkhorik and L.S. Khazan, *Plastic Deformation and Mismatch Dislocations in Heteroepitaxial Systems* (Naukova Dumka, Kyiv, 1983) (in Russian).
23. V.P. Kladko, T.G. Kryshab, G.N. Semenova, L.S. Khazan, and O.S. Bashevskaya, *Fiz. Tverd. Tela* **33**, 3192 (1991).
24. V.P. Kladko, A.V. Kuchuk, N.V. Safryuk, V.F. Machulin, A.E. Belyaev, H. Hardtdegen, and S.A. Vitusevich, *Appl. Phys. Lett.* **95**, 031907(3) (2009).

Received 05.05.09.

Translated from Ukrainian by O.I. Voitenko

ВПЛИВ ДИСЛОКАЦІЙНОЇ
СТРУКТУРИ НА ДЕФОРМАЦІЙНІ ПРОЦЕСИ
В ГЕТЕРОСТРУКТУРАХ $\text{AlGaIn}/\text{GaIn}/(0001)\text{Al}_2\text{O}_3$

В.П. Кладько, А.В. Кучук, Н.В. Сафрук,
О.Є. Беляев, В.Ф. Мачулін

Резюме

У статті представлено результати дослідження структурних властивостей гетеросистем $\text{AlGaIn}/\text{GaIn}/(0001)\text{Al}_2\text{O}_3$ за допомогою високороздільної X-променевої дифрактометрії (ВРХД). На основі отриманих результатів обговорена мікроскопічна природа просторових неоднорідностей у цих структурах (мікродеформації і густина дислокацій). Шляхом чисельного моделювання підтверджено градієнтний розподіл дислокацій і деформацій по глибині як у мозаїчній (блочній) структурі нітридних шарів, так і в області інтерфейсу підкладки сапфіру. Встановлено взаємозв'язок деформацій із густиною дислокацій у шарах і підкладці при зміні товщини останньої. Показано, що збільшення товщини підкладки сапфіру приводить до збільшення пружних деформацій та до зменшення густини дислокацій у шарах структури. Отримано експериментальне підтвердження картини сполучення елементарних комірок шару і підкладки на межі поділу, що приводить до мінімальної невідповідності ґраток.